HHS Public Access

Author manuscript

J Immunol. Author manuscript; available in PMC 2020 June 01.

Published in final edited form as:

J Immunol. 2019 June 01; 202(11): 3173–3186. doi:10.4049/jimmunol.1800943.

A new IRF-1-driven apoptotic pathway triggered by IL-4/IL-13 kills neonatal Th1 cells and weakens protection against viral infection

Mindy M. Miller[*], **Subhasis Barik**[*], **Alexis N. Cattin-Roy**[*], **Tobechukwu K. Ukah**[*], **Christine M. Hoeman**[*], and **Habib Zaghouani**[*,§,¶]

[*]Department of Molecular Microbiology & Immunology, University of Missouri School of Medicine, M616 Medical Sciences Building, Columbia MO 65212, USA.

[¶]Department of Child Health, University of Missouri School of Medicine, M616 Medical Sciences Building, Columbia MO 65212, USA.

[§]Department of Neurology, University of Missouri School of Medicine, M616 Medical Sciences Building, Columbia MO 65212, USA.

Abstract

Early life immune responses are deficient in T helper 1 (Th1) lymphocytes which compromises neonatal vaccination. We found that IL-4 and IL-13 engage a developmentally expressed IL-4Rα/IL-13Rα1 heteroreceptor (HR) to endow interferon regulatory factor 1 (IRF-1) with apoptotic functions which redirect murine neonatal Th1 reactivation to cell death. IL-4/IL-13 induced STAT6 phosphorylation serves to enhance IRF-1 transcription and promotes its egress from the nucleus. In the cytoplasm, IRF-1 can no longer serve as an anti-viral transcription factor but instead co-localizes with Bim and instigates the mitochondrial, or intrinsic, death pathway. The new pivotal function of IRF-1 in the death of neonatal Th1 cells stems from the ability of its gene to bind STAT6 for enhanced transcription and the proficiency of its protein to precipitate Bim-driven apoptosis. This cytokine induced, IRF-1-mediated developmental death network weakens neonatal Th1 responses during early life vaccination and increases susceptibility to viral infection.

Introduction

Landmark observations described early life as a window during which tolerance can be induced to prevent graft rejection (1). Later, however, it was shown that tolerance is not due to an inability of neonates to mount an immune response (2–5), but rather to a deficit in inflammatory Th1 cells and excess in Th2 responses (6–9) which would explain neonatal vulnerability to infections and allergic reactions (10). Fine analysis, however, indicated that the primary neonatal response displays balanced Th1/Th2 cells, while a rechallenge with Ag elicits secondary immunity devoid of Th1 lymphocytes (11, 12). Surprisingly, IL-4 from Th2 cells proved toxic to the Th1 counterparts inducing their death by apoptosis (12). This was

Correspondence to: Habib Zaghouani, The University of Missouri School of Medicine, Department of Molecular Microbiology and Immunology, M616 Medical Sciences Building, 1 Hospital Drive, Columbia, MO 65212. Phone: (573) 884-0659, Fax: (573) 882-4287, zaghouanih@health.missouri.edu.

puzzling as IL-4 does not seem to signal in Th1 cells despite expression of the conventional IL-4 receptor (IL-4Rα/common γ chain) (13). Further studies though demonstrated that primary neonatal Th1 cells unexpectedly up-regulate IL-13Rα1 which associates with IL-4Rα to form an IL-4Rα/IL-13Rα1 heteroreceptor (HR) through which both IL-4 and IL-13 cytokines can signal (12, 14, 15). Remarkably, IL-4 cytotoxicity and death of neonatal Th1 cells were tied to signaling of the cytokines through the HR (12, 15). This is a conundrum as Interleukins usually foster growth rather than cell death and prompts a resolve to untangle the mechanisms underlying IL-4-induced death of neonatal Th1 cells. In this investigation, mouse models were adapted to examine the intracellular molecular networks underlying neonatal Th1 cell death and uncovered a previously unrecognized apoptotic pathway that shifts activation towards mortal cellular programs. Indeed, re-stimulation of primary HR^+ Th1 cells through the TCR in presence of either IL-4 or IL-13 leads to STAT6 phosphorylation resulting in transcriptional activation and nuclear-to-cytoplasm translocation of interferon regulatory factor 1 (IRF-1). Unexpectedly, cytoplasmic IRF-1 triggers a Bim-driven activation of the mitochondrial apoptotic pathway. The consequence of this cytokine-driven IRF-1-mediated Th1 death translates into reduced effectiveness of neonatal vaccination against Lymphocytic Choriomeningitis Virus (LCMV) infection. Moreover, interference with IRF-1 death network by ways of HR ablation or inhibition of downstream signaling restores vaccine effectiveness and protection against viral infection.

Materials and Methods

Mice

Balb/c IL-13Rα1$^{+/+}$ ($HR^{+/+}$) mice were purchased from Harlan Sprague Dawley (Indianapolis, IN). Balb/c IL-13Rα1$^{-/-}$ ($HR^{-/-}$) mice were generated in our laboratory (16). DO11.10/Rag2$^{-/-}$ transgenic mice which express an OVA-specific TCR have been previously described (12). DO11.10/Rag2$^{-/-}$ IL-13Rα1$^{-/-}$ referred to as DO11.10 $HR^{-/-}$ mice were generated by crossing Balb/c $HR^{-/-}$ mice with DO11.10/Rag2$^{-/-}$ mice. IL-13Rα1$^{+/+}$-GFP Balb/c mice, which express green fluorescent protein (GFP) under the IL-13Rα1 promoter were generated in our laboratory as described (17). These mice were crossed onto the DO11.10 Rag2$^{-/-}$ Balb/c background to produce DO11.10 IL-13Rα1-GFP reporter mice referred to as DO11.10-$HR^{+/+}$-GFP. C57BL/6 IL-13Rα1$^{+/+}$ ($HR^{+/+}$) mice were purchased from The Jackson Laboratory (Bar Harbor, ME). C57BL/6 OT-II transgenic mice which express an OVA-specific TCR were previously described (18). C57BL/6 IL-13Rα1$^{-/-}$ ($HR^{-/-}$) mice were generated by crossing the Balb/c $HR^{-/-}$ mice to the C57BL/6 background by speed congenics. C57BL/6 OT-II $HR^{-/-}$ mice were generated by crossing C57BL/6 $HR^{-/-}$ mice to OT-II mice. All mice were bred and maintained in the animal care facility for the duration of the experiments and all experimental procedures were performed according to the guidelines of the University of Missouri Animal Care and Use Committee.

Antigens

OVAp (SQAVHAAHAEINEAGR) corresponding to amino acids 323–339 of chicken OVA and including both OT-II and DO11.10 epitopes was purchased from EZbiolab (Carmel, IN).

Ig-OVA is an IgG2b molecule expressing OVAp within the heavy chain variable region and has been produced in our laboratory (19).

LCMV Viruses and peptides. Both Armstrong and Clone13 viruses were used for challenge to test for vaccine effectiveness in $HR^{-/-}$ relative to $HR^{+/+}$ mice. LCMV glycoprotein (GP) amino acid residues 33–41 (GP33) CD8 T cell epitope and GP 61–80 (GP61) CD4 T cell peptide were obtained from EZBiolab (Carmel, IN) and used in immunization and ex vivo stimulation for analysis of T cell responses.

LCMV GP-specific tetramers. GP33 and GP61 Tetramers were obtained from the NIH Tetramer Core Facility at Emory University (Atlanta, GA).

Neonate-to-neonate T cell transfer

Splenic cells from 1-day-old $HR^{-/-}$ or $HR^{+/+}$ DO11.10 or OT- II donor mice were transferred (3×10^6 cells per mouse) i.v. through the facial vein into 1-day old $HR^{+/+}$ Balb/c or C57BL/6 host mice using a 30 gauge needle as previously described (19). This transfer model increases the frequency and facilitates tracking of responders cells during analysis of the primary responses (12, 19, 20).

Exposure to Ag and viral infection

Neonatal exposure to Ig-OVA. One day-old mice recipient of neonatal splenic T cell transfer were given an intraperitoneal (i.p.) injection of 100 μg Ig-OVA in sterile saline and used for analysis of primary and secondary responses.

Neonatal vaccination with LCMV peptides. Three day-old mice were given i.p. a peptide vaccine consisting of 10μg each of GP33 and GP61 in a 100 μl saline/IFA solution (1 vol/ 1vol) and used later to test for protection against viral infection.

LCMV viral infection. Mice vaccinated with LCMV peptides were infected with either 2×10^5 PFU of Armstrong (i.p.) or 2×10^6 PFU of Clone13 (i.v.) strains.

Analysis of OVA-specific T cell responses

Primary Responses. Two weeks after T cell transfer and exposure to Ig-OVA, the spleen cells were analyzed ex vivo for production of IFNγ and IL-4 cytokines. Briefly the cells were stimulated for four hours with 10μM OVAp in the presence Brefeldin A to accumulate sufficient intracellular cytokines. Subsequently, the cells were stained with antibodies to CD4 and KJ1–26 (DO11.10 T cells) or Vα2/Vβ5 (OT-II T cells) and intracellular cytokines were detected by staining with anti- IFNγ and IL-4 antibodies. Analyses used flow cytometry performed on a Beckman Coulter CyAn (Brea, CA).

Recall Responses. Two weeks after T cell transfer and exposure to Ig-OVA, the spleen cells were stimulated with 10μM OVAp for 48 hours and cytokine secretion was analyzed by ELISA while the frequency of cytokine-producing cells was determined using ELISPOT.

Secondary Responses. Two months after T cell transfer and exposure to Ig-OVA, mice were challenged with 125μg OVAp in CFA. Ten days later, the lymph node (LN) cells were

stimulated with 10μM OVAp for 24 hours and cytokine secretion was analyzed by ELISA while the frequency of cytokine-producing cells was determined using ELISPOT.

Analysis of Apoptosis in primary Th1 cells

Two weeks after T cell transfer and exposure to Ig-OVA, the spleen cells were stimulated with 10μM OVAp for 12h with Brefeldin A (10μg/ml) added during the last 8h of the stimulation. The DO11.10 (KJ1–26$^+$) and OT-II (Vα2$^+$/Vβ5$^+$) Th1 cells (IFNγ$^+$) were analyzed for Annexin V binding by Flow cytometry.

Analysis of LCMV-specific T cell responses

Neonatal mice given GP33/GP61 peptide vaccine and infected with LCMV Arm or CL13 strain at the age of 7 weeks were sacrificed on day 7 and 30 post infection with Arm and CL13, respectively. The frequency of Ag-specific CD4 and CD8 T cells was analyzed by GP33/GP61 Tetramer binding. Ex-vivo intracellular TNFα and IFNγ production by CD4 and CD8 T cells was measured after a brief stimulation (5 hours) with a peptide mixture containing 1 μg/ml GP33 and 5μg/ml GP61 in the presence Brefeldin A.

ELISA and ELISPOT

ELISA. IL-4 and IFNγ production was measured using the standard BD biosciences protocol (San Jose, CA) using anti-cytokine antibodies. The OD450 was read on a SpectraMax 190 counter (Molecular Devices, Sunnyvale, CA) and analyzed using SOFTmax PRO 3.1.1 software. Cytokine concentrations were extrapolated from the linear portion of a standard curve generated by graded amounts of recombinant cytokine.

ELISPOT. HA multiscreen plates (Millipore, Bedford, MA) were coated with capture antibody and free sites were blocked with serum-containing media prior to stimulating cells with 10μM OVAp. Biotinylated antibodies were added and bound antibodies were revealed with avidin peroxidase. Spots were imaged on a CTL Analyzer series 3B (Cleveland, OH) and counted using CTL's Immunospot software version 3.2.

Generation and sorting of neonatal HR$^+$Th1 cells

Two sources were used to sort HR$^+$Th1 cells. Initially, we used primary splenic cells from one day-old mice recipient of neonatal DO11.10 T cell transfer and given 100 μg Ig-OVA as described in analysis of primary responses. In experiments requiring high number of HR$^+$Th1 cells we used primary cells from the following in vitro culture system: Splenocytes which contain both APCs and T cells were harvested from neonatal DO11.10-HR$^{+/+}$-GFP mice and stimulated with 10μM OVAp for 24 hours. Excess OVAp was washed off and the incubation continued for an additional 72 hours. The culture was then stained with anti-CD4 and anti-CD11c antibodies and HR$^+$Th1 cells were sorted as CD11c$^-$CD4$^+$GFP$^+$(HR$^+$) cells. The culture was also used for sorting control CD11c$^+$GFP$^+$ DCs. The sorting was performed on a Beckman Coulter MoFlo (Brea, CA) and only sorts yielding >95% purity were used for experiments.

Analysis of cytokine-induced Th1 death in vitro

Sorted neonatal HR^+CD4^+ Th1 cells are stimulated with 10μg anti-CD3 (10 μg/ml) and anti-CD28 (1 μg/ml) antibodies in the presence of 5U rIL-4 or rIL-13 for 24 or 48 hours. Apoptosis was evaluated by 7-AAD binding to $CD4^+$ T cells by flow cytometry.

Analysis of cytokine-induced proliferation in vitro

Sorted HR^+ neonatal Th1 cells (20,000/well) were labelled with CellTrace Violet (Invitrogen, Carlsbad, CA) according to manufacturer's instructions and incubated with Ag and/or cytokine for 72 hours. Dye dilution, a measure of cell proliferation, was analyzed by flow cytometry.

Western blots

Sorted neonatal HR^+CD4^+ Th1 cells (50×10^3 cells) were stimulated with Ag and cytokine for the indicated amount of time, lysed, run on a 4–12% SDS-PAGE NuPage gradient gel, and transferred to a PVDF membrane. After, saturation with 5% BSA, the membrane was incubated target specific rabbit antibodies (Cell Signaling Technologies, Danvers, MA), and blotted with a secondary anti-rabbit-HRP antibody (CST). The membrane was then incubated with with LI-COR WesternSure Premium substrate (Lincoln, NE) and images were collected on a LI-COR Odyssey Fc. Densitometry analysis was performed with ImageStudioLite v5.2 software (Lincoln, NE).

STAT Inhibition

In vitro. Sorted HR^+CD4^+ neonatal Th1 cells were pretreated for one hour with STAT inhibitors before the addition of antigen and cytokines. The inhibitors were Fludarabine (2.5μM) for STAT1, S3I-201 (100μM) for STAT3 and AS1517499 (200nM) for STAT6. STAT1 and 3 inhibitors were Selleckchem (Houston, TX) and STAT6 inhibitor was from Axon Medchem (Reston, VA).

***In vivo*.** LCMV **v**accinated mice were given i.p. a 10mg/kg STAT6 inhibitor (AS1517499) in 60μl DMSO/PBS (1 vol/1 vol) daily for 5 days starting 2 days prior to viral infection.

RT-qPCR

Sorted HR^+CD4^+ neonatal Th1 cells were stimulated with Ag and cytokine and RNA was isolated with Trizol extraction and ethanol precipitation. Quantitative RT-PCR was performed using the Power SYBR Green RNA-to-CT 1-Step Kit on a StepOnePlus thermocycler (Applied Biosystems, Foster City, CA).

shRNA silencing

Three different 29mer shRNA molecules targeting murine IRF-1 and a scrambled non-specific shRNA molecule were designed using the online RNAi Central program (http://cancan.cshl.edu/RNAi_central/RNAi.cgi?type=shRNA). Sequences were engineered to express the human U6 promotor as well as a loop containing the Sma1 restriction site. Full sequences containing restriction sites, promoter, shRNA palindromes separated by 8nt loop, and transcription end site (referred to as ultramer Oligos) are as follows (5'→3'):

IRF-1 ultramer oligo 1—
AAAGCGGCCGCTTGTGGAAAGGACGAAACACCTGCAGATTAATTCCAACCAAAT
CCCAGGGACCCGGGACCCTGGGATTTGGTTGGAATTAATCTGCATTTTTATCGAT

IRF-1 ultramer oligo 2—
AAAGCGGCCGCTTGTGGAAAGGACGAAACACCCATCGAGGAAGTGAAGGATCAG
AGTAGGAACCCGGGATCCTACTCTGATCCTTCACTTCCTCGATGTTTTTATCGAT

IRF-1 ultramer oligo 3—
AAAGCGGCCGCTTGTGGAAAGGACGAAACACCCACTGTCACCGTGTGTCGTCAG
CAGCAGTACCCGGGAACTGCTGCTGACGACACACGGTGACAGTGTTTTTATCGAT

Scrambled ultramer oligo—
AAAGCGGCCGCTTGTGGAAAGGACGAAACACCGCGCACACCACATTAGTTCGTA
GAACTAAACCCGGGATTAGTTCTACGAACTAATGTGGTGTGCGCTTTTTATCGAT.

The following primers (IDT, San Jose, CA) were used in PCR to amplify the ultramer oligos before cloning into propagation plasmids.

Common Fwd: 5’-AAAGCGGCCGCTTGTGGAAAG-3’

IRF-1 ultramer oligo 1 Rev: 5’-ATCGATAAAAATGCAGATTAATTCCAACCAA-3’

IRF-1 ultramer oligo 2 Rev: 5’-ATCGATAAAAACATCGAGGAAGTGAAGG-3’

IRF-1 ultramer oligo 3 Rev: 5’-ATCGATAAAAACACTGTCACCGTGTG-3’

Scrambled ultramer oligo Rev: 5’-ATCGATAAAAAGCGCACACCACATTAG-3’

The PCR products were T-A cloned into pUC19 for propagation. Upon confirmation by automated sequencing the constructs were individually cloned into the MSCV-IRES-Thy1.1 retroviral vector using Not1 and Cla1 restriction sites and the resulting retroviral vectors were used to transduce sorted HR^+CD4^+ neonatal Th1 cells as described (21).

Chromatin immunoprecipitation (ChIP) assay

This was used to identify STAT6 binding sites in the IRF-1 gene. Sorted HR^+CD4^+ neonatal Th1 cells (100,000 cells/group) were stimulated with Ag + cytokines, fixed/crosslinked in 1% formaldehyde for 10 min and the reaction was quenched with 0.125M glycine. Cells were then lysed with SDS buffer supplemented with protease inhibitors and sonicated on a Misonix 3000 sonicator (Power 5, 5 cycles of 15s on and 60s off) to produce chromatin fragments of 150–500bp. The lysates were then cleared of debris by centrifugation and incubated with protein G coated magnetic beads (CST) to remove non-specific protein binding. The precleared lysate was precipitated overnight with either STAT6 antibody or rabbit IgG isotype and complexes were brought down by incubation with protein G coated magnetic beads. The samples were washed in low salt then high salt buffer and chromatin was eluted in ChIP elution buffer (all buffers from CST SimpleChIP kit). Unprecipitated (5% of total lysate volume) and STAT6-specific chromatin were treated with Proteinase K to

reverse crosslinking and DNA was purified with ChIP DNA Clean and Concentrator kit (Zymo, Irvine, CA). PCR reactions were then performed using the following STAT6 binding site specific primers (5'→3'):

Promoter Fwd: CTTTCCAAGACAGGCAAGG,

Promoter Rev: AACACTTAGCGGGATTCC,

Exon 3 Fwd: TCAGCCTTTTCCCATACTTG,

Exon 3 Rev: CGGAACAGACAGGCATC,

Intron 3 Fwd: TGCAGAATTACTGGAGCAG,

Intron 3 Rev: TTGAGAAAGGAAGATGGAAGTC,

3'UTR Fwd: GATCCTCAGGGAGAGCAG,

3'UTR Rev: TCAGAGGCAGGCAGAG.

Real-time PCR reactions were performed using the SYBR Green Universal Master Mix (Applied Biosystems, Foster City, CA) and % Input was calculated as follows: 5 × 2 ^(C[t]5% Input sample - C[t]IP sample).

Assay for STAT6 binding site specificity

The wild type (IRF-1-WTI3) and either a mutated promoter (MuP-IRF-1) or intron 3 (IRF-1-MuI3) STAT6 binding site IRF-1 genes were separately cloned into the MSCV-IRES-Thy1.1 retroviral vector in front of the mCherry sequence for use as reporters for IRF-1 expression. Specifically, the MSCV-IRES-Thy1.1 retroviral vector was engineered to express the murine IRF1 gene from −406bp to +8,048bp relative to the TSS (GRCm38.p6) with the sequence for mCherry added between the last exon and the 3'UTR. This was done in 2 steps: The 5' end of IRF-1 including the promoter and ORF regions was cloned first and the resulting vector was used to insert downstream the mCherry gene fused with the IRF-1 3' end (3'UTR and flanking sequence). The cloning procedures are as follows: the 5' IRF-1 region was PCR amplified from the murine genome isolated from a tail snip of Balb/c mice using a forward primer to add the Not1 site (5'-AAGCGGCCGCTTCATTACCAGACTGATTTTG-3') and a reverse primer to add the HindIII site (5'-AAAAGCTTTGGTGCACAAGGAATGGCCTGAATAG-3') and cloned into pBluescript SK(+) with HindIII and NotI. mCherry gene was cloned into pUC19 using XbaI/HindIII restriction enzymes. The 3' IRF-1 was PCR amplified from the Balb/c genome using a forward primer (5'-AATCTAGATTTGGGTCTCTGACCCGTTCTTGC-3') that adds an XbaI site and a reverse primer (5'-AAGGATCCGTCGACATTGCCTGCACTGTTGTCTA-3') that adds both EcoR1 and SalI restriction sites. This 3' IRF-1 fragment was cloned into the xbaI/Sal1 site of pUC19 downstream of mCherry gene yielding an 3'IRF-1/mCherry sequence that was cloned into pBluescript/5'IRF1 using HindIII and SalI. The pBluescript plasmid carrying the IRF-1/mCherry fusion gene was then used to generate IRF-1/mCherry sequence with mutated

promoter and Intron 3 STAT6 binding site by site directed mutagenesis utilizing the following primers:

Promoter Fwd: 5’-CTCTACAACAGCCTGATAAACCCGAAATGATGAGGCCGAG-3’

Promoter Rev: 5’-CTCGGCCTCATCATTTCGGGTTTATCAGGCTGTTGTAGAG-3’

Intron 3 Fwd: 5’-CTGTATAGAATACAGGGGCTAGAAAAAACAGTTGTGAGTCAGG-3’

Intron 3 Rev: 5’-CCTGACTCACAACTGTTTTTTCTAGCCCCTGTATTCTATACAG-3’

Three IRF-1/mCherry fusion DNA fragments were cut out from these plasmids and cloned into MSCV-IRES-Thy1.1 retroviral vector yielding viruses carrying the wild type IRF-1-WTI3/mCherry fusion gene as well as viruses carrying fusion fragment with mutated STAT6 binding site within the promoter (MuP-IRF-1/mCherry) and intron 3 (IRF-1-MuI3/mCherry).

Co-Immunoprecipitation

Sorted HR^+CD4^+ neonatal Th1 cells were stimulated for 24 hours with Ag and cytokines, lysed, pre-cleared with rabbit IgG and protein G Sepharose beads (Invitrogen, Carlsbad, CA) and incubated with anti-Bim or anti-IRF1 antibodies (CST, Danvers, MA). Subsequently, protein G Sepharose beads were added and Bim/IRF-1-Abs complexes were pulled down by centrifugation. The supernatant was further used for an additional immunoprecipitation with anti-beta-tubulin to obtain Tubulin-Abs complexes. Samples were analyzed by western blot.

Confocal microscopy

Sorted HR^+CD4^+ neonatal Th1 cells were stimulated with Ag and cytokine for 24 hours and spun onto glass slides using a StatSpin Cytofuge 2 (Iris Sample Processing, Westwood, MA). Cells were fixed in methanol and stained with primary anti-IRF1 (CST) and Alexa647-conjugated anti-Bim (Novus) antibodies. Secondary Alexa555-conjugated anti-rabbit antibody was used to detect IRF-1. The slides were then mounted with fluoroshield mounting medium with DAPI (Abcam) and imaged on a Leica TCP SP8 confocal microscope at 63x magnification and processed with LAS X software (Leica, Wetzlar, Germany).

Yeast-two-hybrid

Assessment of Bim and IRF1 interaction was performed using the ProQuest Two-Hybrid System (Invitrogen, Carlsbad, CA). To generate IRF-1, Bim, and Bcl-2 sequences, mRNA was isolated from a Balb/c mouse spleen, cDNA synthesized using RevertAid First Strand Synthesis cDNA kit (Thermo) and amplified by PCR using primers that include attB sites, Shine-Dalgarno, and Kozak sequences as follows (5’→3’):

IRF1 Fwd: GGGGACAAGTTTGTACAAAAAAGCAGGCTTCGAAGGAGATAGAAC

CATGCCAATCACTCGAATGCGGATGA

IRF1 Rev: GGGGACCACTTTGTACAAGAAAGCTGGGTCCTATGGTGCACAAGGA ATGGCCTGA

Bim Fwd: GGGGACAAGTTTGTACAAAAAAGCAGGCTTCGAAGGAGATAGAAC CATGGCCAAGCAACCTTCTGATGTAA

Bim Rev: GGGGACCACTTTGTACAAGAAAGCTGGGTCTCAATGCCTTCTCCATA CCAGACGG

Bcl-2 Fwd: GGGGACAAGTTTGTACAAAAAAGCAGGCTTCGAAGGAGATAGAAC CATGGCGCAAGCCGGGAGAACAGGGT

Bcl-2 Rev: GGGGACCACTTTGTACAAGAAAGCTGGGTTCACTTGTGGCCAGGTA TGCACCC.

Entry clones were generated in pDONR plasmid by BP recombination using the Gateway Technology Clonase II kit (Invitrogen) and sequences confirmed by automated sequencing. Bait and prey plasmids were then generated in pDest32 by LR recombination. MAV203 yeast cells were transformed with different combinations of bait and prey plasmids and transformants were assessed for protein-protein interaction by β-galactosidase assay. Quantitative liquid culture β-galactosidase assay was performed by growing the transformants in YPD medium until mid-log phase, recording the OD600, lysing the cells by rapid freeze/thaw cycles in Z buffer, and incubating with ONPG substrate until yellow color developed. The elapsed time for color development and the final OD420 was used to determine β-galactosidase units with the following formula: units = 1,000 x OD420/(time x volume of cells x OD600).

Plaque assays for analysis of viral titers

Vero E6 cells (ATCC, Manassas, VA) were grown to 95% confluency in 6-well plates and infected for 90 minutes with dilutions of homogenized tissue and serum samples. To allow plaque formation, the samples were aspirated, cells overlayed with agarose + EMEM, and incubated for 7 days. The samples were then fixed with formaldehyde, the agarose overlay removed and stained with crystal violet to visualize plaques.

Results

IL-4/IL-13 signaling in Th1 cells shifts Ag-induced activation towards apoptosis

During rechallenge with Ag, neonatal Th2 cells produce IL-4 which signals through the HR and drives apoptosis of the Th1 counterparts (10). However, it is not known whether IL-4 signaling causes Th1 death by directly triggering the apoptotic pathway or by interfering with Ag stimulation to shift reactivation toward death. To address this question we began by generating HR-expressing Ovalbumin 323–339 (OVAp)-specific primary neonatal DO11.10 Th1 cells (referred to as $CD4^+HR^+$ Th1 cells) by exposure of IL-13Rα1-GFP TCR_{OVA}

DO11.10 T cells to Ig-OVA *in vivo* or OVAp *in vitro* as described in Materials and Methods. Because neonatal exposure to Ig-OVA or OVAp leads to up-regulation of IL-13Rα1 only in Th1 cells (12, 15, 17, 20) sorting of these Th1 cells was performed on the basis of GFP (IL-13Rα1) expression. As expected the purified cells express IL-13Rα1 protein on the surface and the Th1-specific Tbet transcription factor (Fig. S1). All other transcription factors were at background level indicating that the sorted cells represent $CD4^+HR^+$ neonatal Th1 cells. These observations confirm our previous studies that neonatal immunization leads to IL-13Rα1 up-regulation only on Th1 cells(12, 15, 17, 20). It should be noted that polarized Th17 cells from adult subjects are able to up-regulate IL-13Rα1 (22, 23). These $CD4^+HR^+$ neonatal TCR_{OVA} Th1 cells were then tested for apoptosis upon stimulation with anti-CD3/anti-CD28 antibodies and/or cytokines. Because the cells are OVA-specific T cells and stimulation with anti-CD3/anti-CD28 antibodies mimics Ag by inducing signaling through the TCR we refer to it as Ag stimulation. These cells were then used to analyze apoptosis upon stimulation with Ag and/or cytokines. The results indicate that when neonatal $CD4^+HR^+$ Th1 cells are stimulated with IL-4 or IL-13 without Ag apoptosis was at background levels similar to No Ag or cytokine (Figure 1A). Likewise, stimulation with Ag without cytokine also yielded background levels of apoptosis. However, when the stimulation was carried out with Ag and IL-4 or IL-13, there was 40 and 38% cell death, respectively (Figure 1A). Combined results from three independent experiments indicate that the data is statistically significant (Figure 1B). Further analyses indicated that stimulation with Ag induces activation/proliferation of the Th1 cells while IL-4 or IL-13 does not (Figure 1C). However, when the cytokines are added to the culture about half of the cells fail to proliferate. Interestingly, the cells that could not proliferate due to cytokine addition are undergoing cell death (Figure 1D). Indeed, the percentage of cell death was significantly higher among non-proliferating versus proliferating cells (Figure 1E) indicating that IL-4 and IL-13 target activated cells to induce death. In all, IL-4 and IL-13 shifts Ag-restimulation from activation to death.

IL-4/IL-13 signaling through the HR activates STAT6 to drive Th1 death

Signaling through the conventional IL-4 receptor is relatively well defined (24) while signaling through the HR is being elucidated (25) and remains in its infancy for neonatal Th1 cells. The common most proximal signaling mediators for cytokine receptors involve JAK/STAT molecules. Therefore, we began by assessing the dying Th1 cells for phosphorylation of STAT proteins. Figure 2A shows that the cells display basal phosphorylation of $STAT1^{Y701,\ S727}$ and $STAT3^{Y705,\ S727}$ but not $STAT6^{Y641}$ without stimulation with Ag or cytokines. This status remains unchanged when the cells are stimulated with Ag alone. However, the addition of IL-4 or IL-13 alongside Ag increased phosphorylation of $STAT6^{Y641}$ only. Compiled results from 3 independent experiments indicate that the enhanced $STAT6^{Y641}$ activation is statistically significant relative to stimulation with Ag alone (bar graphs in Figure 2A). Note that $STAT6^{Y641}$ phosphorylation is more prominent with IL-4 relative to IL-13. These results are supported by the findings that neither STAT1 nor STAT3 inhibitor is able to block death of Th1 cells whereas STAT6 inhibition rescues the cells from apoptosis as evident by minimal 7-AAD staining (Figure 2B). Data compiled from 3 independent experiments demonstrate that protection of Th1 cells from death by STAT6 inhibitor is statistically significant (Figure 2C). Moreover,

STAT6 activation in the rescued Th1 cells is reduced dramatically by the inhibitor and went down from 664 to 21 arbitrary densitometry units when STAT6 inhibitor was added alongside Ag and IL-4/IL-13 cytokine (Figure 2D), further indicating that STAT6 plays a critical role in IL-4/IL-13 driven Th1 apoptosis. Overall, the fact that death of neonatal Th1 cells is specifically tied to STAT6 activation bodes well with observations in Th17 cells showing that STAT1 activation by HR signaling affects the function rather than the survival of the target (Th17) cells (26).

IRF-1 up-regulation is required during neonatal Th1 apoptosis

Since neonatal Th1 cells die by apoptosis we sought to determine whether STAT6 drives cell death through the intrinsic (mitochondrial) or extrinsic pathway (27). To this end, gene expression analysis of key molecules involved in either pathway was performed in the dying cells. The results demonstrate that the expression of several key intrinsic apoptotic molecules was upregulated in the dying Th1 cells while only IRF-1 (28), a transcription factor known to regulate the extrinsic pathway (29) was increased (Figure S2). Indeed, this gene expression profile manifests in dying Th1 cells as a consequence of stimulation with Ag and IL-4 or IL-13 but not in unstimulated cells or those stimulated with Ag only. Adult Th1 cells, which do not express the HR, or neonatal DCs which express the HR did not display such gene expression profile under any stimulation condition (Figure S2). Surprisingly, however, IRF-1 mRNA upregulation was not accompanied by increased expression of its transcriptional targets, TRAIL (30) and FasL (29). To ensure that IRF-1 is functional and plays a role in the death of Th1 cells we sought to determine whether mRNA up-regulation translates into increased protein levels that would be required for Th1 apoptosis. Indeed, neonatal Th1 cells that were not stimulated with Ag or cytokines display a basal level of IRF-1 protein which is required for naïve to Th1 differentiation during the initial Ag priming (Figure 3A). This basal IRF-1 protein level was not affected upon stimulation with Ag alone (Figure 3A). However, IRF-1 protein level increased significantly when the Th1 cells were stimulated with Ag in the presence of either IL-4 or IL-13 (Figure 3A). More important, to demonstrate that IRF-1 is required for apoptosis the Th1 cells were infected with a retrovirus encoding an IRF-1-shRNA cocktail prior to rechallenge with Ag and cytokines, The results show that the IRF-1 increase was nullified (Figure 3B) and consequently, death of the Th1 cells was significantly decreased (Figure 3C). In all, IL-4/IL-13 signaling in Th1 cells increased IRF-1 expression which is required for cell death.

IL-4/IL-13-induced pSTAT6 binds specifically to intron 3 DNA sequence of IRF-1 gene during Th1 death

In dying neonatal Th1 cells, STAT6 phosphorylation coincides with IRF-1 upregulation. The two events seem to be tied together as inhibition of STAT6 (STAT6 I) prevented IL-4 and IL-13-induced IRF-1 upregulation during Ag stimulation (Figure 3D). Since STAT6 functions as a transcription factor it is logical to envision a protein-DNA interaction between STAT6 and the IRF-1 gene. To test this premise, we began searching for STAT6-binding sites within the IRF-1 gene (covering DNA sequences 1000bp upstream and downstream the transcription start and end sites, respectively) using the consensus TTC($N_{3–4}$)GAA sequence (31). As indicated in Figure 3E (gene map), four potential sites were identified within the promoter, Exon 3, Intron 3 and the 3’ UTR which were referred to as P, E3, I3 and 3’UTR,

respectively. Chromatin immunoprecipitation (ChIP) assays show that Ag stimulation in presence of IL-4 induces STAT6 binding to only the I3 site within the IRF-1 gene (Figure 3F). This interaction was confirmed by Ag stimulation in the presence of the other Th1 death inducing cytokine, IL-13, which also led to STAT6 binding to I3 in a similar fashion to IL-4 (Figure 3G). STAT6 interaction with I3 binding site is specific because neonatal T cells retrovirally (RV) forced to express a fusion IRF-1/mCherry reporter gene carrying mutated I3 STAT6 binding site (IRF-1-MuI3/mCherry-RV) produce decreased mCherry IRF-1 reporter protein upon Ag and cytokine treatment relative to Th1 cells transduced with IRF-1-WTI3/mCherry-RV a retrovirus carrying the wild type I3 STAT6 binding site or MuP-IRF-1/mCherry-RV which harbors a mutated putative STAT6 binding site in the promoter (Figure 3H, left panel). Data from three independent experiments show that the results are statistically significant (Figure 3H, right panel). Thus, STAT6 binds to I3 of the IRF-1 gene and induces IRF-1 expression.

IRF-1 translocates to the cytoplasm and colocalizes with Bim in dying Th1 cells

Live neonatal Th1 cells express basal levels of IRF-1 perhaps because this transcription factor plays a role in T cell differentiation (32). Surprisingly, though, STAT6 further increased expression of IRF-1 during Th1 cell death (Figure 3). Given that the intrinsic apoptotic pathway is active in dying Th1 cells (Figure S2) and that IRF-1 is required for such death (Figure 3), it is logical to envision cross-talk between IRF-1 and essential molecules of the intrinsic pathway such as Bim. To this end, co-immunoprecipitation assays were performed to determine whether the two molecules interact with one another. The findings show that Bim immunoprecipitation pulls down IRF-1 only upon stimulation of neonatal Th1 cells with Ag and either IL-4 or IL-13 (Figure 4A, left panel). Similarly, IRF-1 immunoprecipitation pulls down Bim under the same Ag and cytokine stimulation (Figure 4A, right panel). Note that the Bim extra-long isoform (Bim_{EL}) but not Bim long (Bim_L) or Bim short (Bim_S) co-precipitate with IRF-1. As Bim is a mitochondrial-associated protein, while IRF-1 usually resides in the nucleus, for co-immunoprecipitation to occur the two molecules must co-localize to interact with one another. Indeed, confocal microscopy analysis shows that during neonatal Th1 death, IRF-1 translocates from the nucleus to the cytoplasm where it co-localizes with Bim (Figure 4B). IRF-1 translocation and co-localization with Bim occur only when the cells are triggered to die by stimulation with Ag and IL-4 or IL-13. Interestingly, inhibition of STAT6 activation during stimulation with Ag and cytokines nullifies IRF-1 translocation to the cytoplasm and co-localization with Bim (Figure 4B). Data compiled from several experiments indicate that during stimulation with Ag alone the majority of neonatal Th1 cells display a nuclear localization of IRF-1 while addition of either IL-4 or IL-13 alongside Ag shifts IRF-1 distribution to the cytoplasm in most (~ 75%) of the cells (Figure 4C). Such a shift, however, did not occur in most of the Th1 cells when Ag and cytokine stimulation is accompanied by STAT6 inhibitor (Figure 4C). As IRF-1 translocates to the cytoplasm, co-localizes and co-immunoprecipitates with Bim, it is possible that the two factors either bind to one another or interact through components of a protein complex. Yeast-two-hybrid system analysis, however, indicates that IRF-1 and Bim do not bind one another directly (Figure S3). Indeed, beta-galactosidase activity (blue colonies) was not observed in Bim/IRF-1 transformants while the internal (Krev1/RalGDS-wt) and experimental (Bcl2/Bim) controls displayed blue colonies (Figure

S2A). Quantitative beta-galactosidase assay revealed a similar trend where only the strong positive Krev1 control and Bcl2/Bim control displayed enzymatic activity but not the test sample Bim/IRF1 (Figure S2B). These results suggest that Bim and IRF-1 do not directly bind one another but likely form a complex with other proteins. Together, these results indicate that during IL-4/IL-13 triggered neonatal Th1 cell death IRF-1 relocates to the cytoplasm and colocalizes with Bim to bridge the intrinsic and extrinsic apoptotic pathways.

Overall, the data suggest that Ag stimulation triggers IRF-1 expression and STAT6-activation by IL-4/IL-13 signaling sustains translocation from the nucleus to cytoplasm leading to Bim-mediated death of Th1 cells

Upon priming with Ag C57BL/6 like Balb/c newborns develop HR-bearing primary Th1 cells that undergo cell death during a later rechallenge with the same Ag

We have previously shown that newborn Balb/c mice (H-2^d) recipient of neonatal OVAp-specific DO11.10 T cells (H-2^d) develop balanced Th1 and Th2 primary responses (12, 20). However, rechallenge with the same Ag later induced death of Th1 cells leading to Th2-biased secondary responses (12). The death of Th1 cells was dependent on HR expression as cell death was nullified in HR-deficient ($HR^{-/-}$) mice and Th1/Th2 balanced secondary immunity was restored (15). Whether the T cell bias and its dependency on HR expression reflect a genetic trait of the Th2-dominant Balb/c strain or represents a broad neonatal attribute remains unknown. To test this premise, we used the Th1-prone C57BL/6 strain (H-2^b) and assayed for development of neonatal responses under HR-sufficient ($HR^{+/+}$) as well as HR-deficient ($HR^{-/-}$) circumstances. To this end, one-day-old C57BL/6 newborns were adoptively transferred with neonatal OVAp-specific OT-II T cells (H-2^b) from $HR^{+/+}$ or $HR^{-/-}$ OT-II mice and the hosts were given Ig-OVA, an Ig molecule carrying OVAp (19) to serve as Ag. The findings indicate that primary neonatal OT-II T cells whether from $HR^{+/+}$ or $HR^{-/-}$ mice, like those from the DO11.10/Balb/c transfer system, develop balanced Th1 and Th2 responses as measured by intracellular IFNγ and IL-4, respectively (Figure 5A). Furthermore, Th1 cells whether OT-II or DO11.10 cells from $HR^{+/+}$ mice undergo apoptosis when recalled with OVAp while those from $HR^{-/-}$ mice had reduced apoptotic activity indicating dependency of Th1 death on HR expression (Figure 5B). This data bodes well with the findings showing that recall with OVAp nullifies IFNγ production by Th1 cells from $HR^{+/+}$ but not from $HR^{-/-}$ mice (Figure 5C). This Th2 skewing and it dependency on HR expression by Th1 cells is also evident in *in vivo* secondary responses (Figure 5D). Overall, the results indicate that Th1 death, its dependency on HR expression and the resulting Th2 bias represents a broad neonatal attribute rather than a strain-specific genetic trait. This offers the opportunity to utilize the well characterized C57BL/6 LCMV infection system to evaluate the effect of Th1 death on vaccination and protection from viral challenge.

Ablation of HR increases effectiveness of neonatal vaccination

Specific ablation of the HR in monoclonal T cells, whether of Balb/c or C57BL/6 origin, preserves primary neonatal Th1 cells and nullifies the bias of secondary responses (Figure 5). We then interrogated these observations for relevance to neonatal vaccination and protection against microbial infection under circumstances that integrate the entire T cell

repertoire. To this end, $HR^{+/+}$ and $HR^{-/-}$ C57BL/6 mice were neonatally vaccinated with a mixture of LCMV GP33–41 (CD8 T cell epitope) and GP61–80 (CD4 T cell epitope) peptides (LCMVp), challenged with LCMV Armstrong 7 weeks later, and protection against acute infection was analyzed. The findings indicate that while both $HR^{+/+}$ and $HR^{-/-}$ mouse strains had decreased virus titers in different susceptible organs (Figure S4A), protection was more effective in $HR^{-/-}$ relative to $HR^{+/+}$ mice as is evident by significant decrease of viral titers in most of the organs (Figure S4B). However, the frequency of Ag-specific $CD4^+$ and $CD8^+$ T cells (Figure S4C) as well as IFNγ and TNFα (Figure S4D) responses were similar in both strain. Thus, the discrepancy in viral titers among $HR^{+/+}$ and $HR^{-/-}$ is perhaps related to differences in innate rather Th1 adaptive immunity, especially that the Arm strain usually causes only acute infection (33). Since the HR affects neonatal Th1 cells, we sought to test for protection against LCMV CL13, a strain that causes chronic infection and viral clearance likely relies more on adaptive immunity. Accordingly, mice neonatally vaccinated with LCMVp were challenged with LCMV CL13 at the age of 7 weeks and assessed for development of secondary CD4 and CD8 T cell responses and protection from infection. The results show that both vaccinated $HR^{+/+}$ and $HR^{-/-}$ mice had reduced virus titers relative to non-vaccinated mice (Figure 6A). However, protection from infection was more effective in $HR^{-/-}$ mice as the titers decreased from 1150 ± 477 to 460 ± 115 pfus/ml in $HR^{+/+}$ relative to $HR^{-/-}$ mice on day 7 post infection (Figure 6B). Viral titer were not significantly different on day 14 and 21. This differential protection is likely due to better secondary T cell responses as the frequency of Ag-specific $CD4^+$GP61 Tet^+ cells and $CD8^+$GP33 Tet^+ T cells was significantly higher in $HR^{-/-}$ relative to $HR^{+/+}$ mice (Figure 6C). Interestingly, while the frequency of IFNγ- and TNFα-producing CD8 T cells was similar in $HR^{-/-}$ and $HR^{+/+}$ mice, the percentages of IFNγ- and TNFα-producing CD4 T cells were significantly higher in $HR^{-/-}$ relative to $HR^{+/+}$ mice (Figure 6D). Taken together, these results further identify the HR as the culprit in poor neonatal vaccine responses.

As the HR signals IRF-1 nucleus-to-cytoplasm translocation and Th1 death through STAT6 activation, blockade of this pathway by STAT6 inhibitor (STAT6 I) would restore Th1 responses and protect against viral infection. To test this premise, neonatal C57BL/6 mice were vaccinated with LCMVp as in Figure 6, and 7 weeks later were given a 5-day STAT6 inhibitor regimen. On day 3 of STAT6 I treatment, the mice were challenged with LCMV CL13 and virus titers in the sera, as well as T cell responses, were measured thereafter. The findings indicate that STAT6 inhibition resulted in a drastic reduction in virus titers early after infection while the control (Nil) mice took 21 days to reach a similar reduction in virus titers (Figure 7A). Furthermore, STAT6 inhibition yielded a significant increase in the frequency of Ag-specific GP61 Tet^+ CD4 and GP33 Tet^+ CD8 T cells relative to control mice which did not receive STAT6 I (Figure 7B). The increase in T cell frequency was accompanied by an increase in the percentage of IFNγ- and TNFα-producing CD4 T cells in STAT6 I-recipients as compared to Nil mice (Figure 7C). These results indicate that signaling through the HR and IRF-1 translocation to the cytoplasm are detrimental to neonatally primed Th1 cells and vaccination in infant mice.

Discussion

Priming with Ag at the neonatal stage, in most cases, compromises the outcome of secondary responses upon rechallenge with same Ag as Th1 cells undergo cell death while Th2 lymphocytes thrive (10). The IL-4/IL-13 HR is central to this immune defect which manifests in different mouse strains regardless of their genetic background. Indeed, both C57BL/6 and Balb/c mice had Th2 biased secondary responses due to Th1 cell death orchestrated by the HR and its cytokine ligands, IL-4 and IL-13. Under these circumstances STAT6 is specifically activated and, unexpectedly, triggers upregulation of IRF-1, a transcription factor known to regulate interferon responses (28). More intriguing, the death of Th1 cells was dependent on IRF-1 expression and its translocation from the nucleus to the cytoplasm. In fact, a STAT6 binding site within the intron, not the promoter (34, 35) of IRF-1 was identified that was tied to IRF-1 transcription and ultimately its translocation from the nucleus to the cytoplasm. Contrary to STAT6 binding to the promoter in mouse macrophages (34) and human cell lines (35), which suppresses IRF-1 transcription, we demonstrate that STAT6 binding to the intron region in neonatal Th1 cells increases IRF-1 transcription. STAT6 may bind to the promoter region of IRF-1 during priming with Ag and differentiation of naïve neonatal T cells into Th1 cells. However, during rechallenge of the Th1 cells with Ag in the presence of cytokines only STAT6 binding to intron 3 seems to be operative as demonstrated by ChIP assay and further confirmed by promoter site mutation which did not affect IRF-1 expression. While the findings highlight STAT6 binding to intron 3 as a major transcriptional regulator of IRF-1 expression during Ag/cytokine induced death of neonatal Th1 cells, it remains to be determined whether other STAT6 binding sites distal to the IRF-1 gene contribute to this outcome. These observations are novel and reveal that STAT6, on the one hand, is identified as an enhancer for IRF-1 transcription in neonatal Th1 cells and, on the other hand, leads to IRF-1 translocation by a yet undefined mechanism. Under these circumstances, IRF-1 nuclear export may be mediated by CRM1 as is the case for IRF-5 (36). Whether IRF-1 translocation is directly regulated by STAT6 or by its transcriptional targets remains unknown. The other perplexing observation is that IRF-1, a member of the extrinsic apoptotic pathway, did not regulate the expression of its normal targets TRAIL and FasL despite being involved in the death of neonatal Th1 cells. Instead, IRF-1 moved to the cytoplasm in a STAT6 dependent manner to co-localize with Bim, a member of the intrinsic apoptotic pathway. While IRF-1 and Bim co-localize and co-precipitate together, their interaction does not seem to be direct and must occur through intermediate proteins. It is likely that IRF-1 tips the scales of the entire mitochondrial apoptotic complex towards death perhaps by binding the anti-apoptotic molecule Bcl2 which would then release Bim (37) to initiate the death cascade. Together, the data highlight a new function for IRF-1 whereby a factor known to control viral infection (38) is turned into a killer of neonatal Th1 cells by merging two apoptotic pathways. Whether, neonatal Th1 cells emanating from CXCL8 producing T cells (39, 40) escape HR up-regulation during such a transition to avoid IRF-1-driven apoptotic pathway remains to be determined.

The functional consequence of the new HR-initiated, IRF-1-driven developmental apoptotic pathway translates into impoverishment of neonatal vaccine effectiveness as demonstrated by enhanced protection against LCMV infection in mice where the HR is non-functional.

Indeed, despite the fact that the vaccine incorporates both CD4 and CD8 T cell epitopes while HR signaling triggers death of Th1 cells only, the differential protection against LCMV CL13 between $HR^{+/+}$ and $HR^{-/-}$ mice, while seems modest, remains significant. In addition, viral protection was assessed at adult age, long after neonatal vaccination, a time during which naïve T cells that are not subject to HR signaling would have accumulated. These cells would contribute primary responses and virus clearance, hence reducing the negative impact of vaccine-induced HR-compromised Th1 (memory) cells. Finally, it remains to be seen whether probiotics and commensal TLRs (41, 42) would trigger DCs to produce sufficient IL-12 that would counter IL-13Rα1 (HR) upregulation on Th1 cells during neonatal vaccination and circumvent IRF-1 apoptotic pathway during microbial infection. Overall, the HR/IRF-1 mediated developmental apoptotic pathway undermines effectiveness of neonatal vaccination.

Supplementary Material

Refer to Web version on PubMed Central for supplementary material.

ACKNOWLEDGEMENTS

We would like to thank Dr. Bumsuk Hahm and the late Dr. Michael P. Sherman for their advice and support on this work.

Funding. This work was supported by grants RO1 AI048541 and R21 HD060089 from the National Institutes of Health (to H.Z.), funds from the Leda J. Sears Trust, and the J. Lavenia Edwards Endowment. M.M.M. was supported by T32 Training Grant GM008396 from the National Institute of General Medical Sciences and by the Research Board grant from the University of Missouri.

Abbreviations:

ChIP	chromatin immunoprecipitation
HR	IL-13Rα1/IL-4Rα heteroreceptor
IP	immunoprecipitation
IRF-1	interferon regulatory factor 1
LCMV	Lymphocytic Choriomeningitis virus

References

1. Billingham RE, Brent L, and Medawar PB. 1953 Actively acquired tolerance of foreign cells. Nature 172: 603–606. [PubMed: 13099277]
2. Qin YF, Sun DM, Goto M, Meyermann R, and Wekerle H. 1989 Resistance to experimental autoimmune encephalomyelitis induced by neonatal tolerization to myelin basic protein: clonal elimination vs. regulation of autoaggressive lymphocytes. Eur J Immunol 19: 373–380. [PubMed: 2467819]
3. Forsthuber T, Yip HC, and Lehmann PV. 1996 Induction of TH1 and TH2 immunity in neonatal mice. Science 271: 1728–1730. [PubMed: 8596934]
4. Ridge JP, Fuchs EJ, and Matzinger P. 1996 Neonatal tolerance revisited: turning on newborn T cells with dendritic cells. Science 271: 1723–1726. [PubMed: 8596932]

5. Sarzotti M, Robbins DS, and Hoffman PM. 1996 Induction of protective CTL responses in newborn mice by a murine retrovirus. Science 271: 1726–1728. [PubMed: 8596933]
6. Powell TJ Jr., and Streilein JW. 1990 Neonatal tolerance induction by class II alloantigens activates IL-4-secreting, tolerogen-responsive T cells. J Immunol 144: 854–859. [PubMed: 2136901]
7. Chen N, and Field EH. 1995 Enhanced type 2 and diminished type 1 cytokines in neonatal tolerance. Transplantation 59: 933–941. [PubMed: 7535960]
8. Singh RR, Hahn BH, and Sercarz EE. 1996 Neonatal peptide exposure can prime T cells and, upon subsequent immunization, induce their immune deviation: implications for antibody vs. T cell-mediated autoimmunity. J Exp Med 183: 1613–1621. [PubMed: 8666919]
9. Min B, Legge KL, Pack C, and Zaghouani H. 1998 Neonatal exposure to a self-peptide-immunoglobulin chimera circumvents the use of adjuvant and confers resistance to autoimmune disease by a novel mechanism involving interleukin 4 lymph node deviation and interferon gamma-mediated splenic anergy. J Exp Med 188: 2007–2017. [PubMed: 9841915]
10. Zaghouani H, Hoeman CM, and Adkins B. 2009 Neonatal immunity: faulty T-helpers and the shortcomings of dendritic cells. Trends Immunol 30: 585–591. [PubMed: 19846341]
11. Adkins B, and Du RQ. 1998 Newborn mice develop balanced Th1/Th2 primary effector responses in vivo but are biased to Th2 secondary responses. J Immunol 160: 4217–4224. [PubMed: 9574522]
12. Li L, Lee HH, Bell JJ, Gregg RK, Ellis JS, Gessner A, and Zaghouani H. 2004 IL-4 utilizes an alternative receptor to drive apoptosis of Th1 cells and skews neonatal immunity toward Th2. Immunity 20: 429–440. [PubMed: 15084272]
13. Huang H, and Paul WE. 1998 Impaired interleukin 4 signaling in T helper type 1 cells. J Exp Med 187: 1305–1313. [PubMed: 9547341]
14. Dhakal M, Hardaway JC, Guloglu FB, Miller MM, Hoeman CM, Zaghouani AA, Wan X, Rowland LM, Cascio JA, Sherman MP, and Zaghouani H. 2014 IL-13Ralpha1 is a surface marker for M2 macrophages influencing their differentiation and function. Eur J Immunol 44: 842–855. [PubMed: 24281978]
15. Dhakal M, Miller MM, Zaghouani AA, Sherman MP, and Zaghouani H. 2015 Neonatal Basophils Stifle the Function of Early-Life Dendritic Cells To Curtail Th1 Immunity in Newborn Mice. J Immunol 195: 507–518. [PubMed: 26034171]
16. Haymaker CL, Guloglu FB, Cascio JA, Hardaway JC, Dhakal M, Wan X, Hoeman CM, Zaghouani S, Rowland LM, Tartar DM, VanMorlan AM, and Zaghouani H. 2012 Bone marrow-derived IL-13Ralpha1-positive thymic progenitors are restricted to the myeloid lineage. J Immunol 188: 3208–3216. [PubMed: 22351937]
17. Hoeman CM, Dhakal M, Zaghouani AA, Cascio JA, Wan X, Khairallah MT, Chen W, and Zaghouani H. 2013 Developmental expression of IL-12Rbeta2 on murine naive neonatal T cells counters the upregulation of IL-13Ralpha1 on primary Th1 cells and balances immunity in the newborn. J Immunol 190: 6155–6163. [PubMed: 23650613]
18. Barnden MJ, Allison J, Heath WR, and Carbone FR. 1998 Defective TCR expression in transgenic mice constructed using cDNA-based alpha- and beta-chain genes under the control of heterologous regulatory elements. Immunol Cell Biol 76: 34–40. [PubMed: 9553774]
19. Li L, Legge KL, Min B, Bell JJ, Gregg R, Caprio J, and Zaghouani H. 2001 Neonatal immunity develops in a transgenic TCR transfer model and reveals a requirement for elevated cell input to achieve organ-specific responses. J Immunol 167: 2585–2594. [PubMed: 11509599]
20. Lee HH, Hoeman CM, Hardaway JC, Guloglu FB, Ellis JS, Jain R, Divekar R, Tartar DM, Haymaker CL, and Zaghouani H. 2008 Delayed maturation of an IL-12-producing dendritic cell subset explains the early Th2 bias in neonatal immunity. J Exp Med 205: 2269–2280. [PubMed: 18762566]
21. Barik S, Miller MM, Cattin-Roy AN, Ukah TK, Chen W, and Zaghouani H. 2017 IL-4/IL-13 Signaling Inhibits the Potential of Early Thymic Progenitors To Commit to the T Cell Lineage. J Immunol 199: 2767–2776. [PubMed: 28893952]
22. Newcomb DC, Zhou W, Moore ML, Goleniewska K, Hershey GK, Kolls JK, and Peebles RS Jr. 2009 A functional IL-13 receptor is expressed on polarized murine CD4+ Th17 cells and IL-13 signaling attenuates Th17 cytokine production. J Immunol 182: 5317–5321. [PubMed: 19380778]

23. Newcomb DC, Boswell MG, Zhou W, Huckabee MM, Goleniewska K, Sevin CM, Hershey GK, Kolls JK, and Peebles RS Jr. 2011 Human TH17 cells express a functional IL-13 receptor and IL-13 attenuates IL-17A production. J Allergy Clin Immunol 127: 1006–1013 e1001–1004. [PubMed: 21236478]
24. Nelms K, Keegan AD, Zamorano J, Ryan JJ, and Paul WE. 1999 The IL-4 receptor: signaling mechanisms and biologic functions. Annu Rev Immunol 17: 701–738. [PubMed: 10358772]
25. Wills-Karp M, and Finkelman FD. 2008 Untangling the complex web of IL-4- and IL-13-mediated signaling pathways. Sci Signal 1: pe55. [PubMed: 19109238]
26. Newcomb DC, Boswell MG, Huckabee MM, Goleniewska K, Dulek DE, Reiss S, Lukacs NW, Kolls JK, and Peebles RS Jr. 2012 IL-13 regulates Th17 secretion of IL-17A in an IL-10-dependent manner. J Immunol 188: 1027–1035. [PubMed: 22210911]
27. Roy S, and Nicholson DW. 2000 Cross-talk in cell death signaling. J Exp Med 192: F21–25. [PubMed: 11034612]
28. Miyamoto M, Fujita T, Kimura Y, Maruyama M, Harada H, Sudo Y, Miyata T, and Taniguchi T. 1988 Regulated expression of a gene encoding a nuclear factor, IRF-1, that specifically binds to IFN-beta gene regulatory elements. Cell 54: 903–913. [PubMed: 3409321]
29. Chow WA, Fang JJ, and Yee JK. 2000 The IFN regulatory factor family participates in regulation of Fas ligand gene expression in T cells. J Immunol 164: 3512–3518. [PubMed: 10725705]
30. Park SY, Seol JW, Lee YJ, Cho JH, Kang HS, Kim IS, Park SH, Kim TH, Yim JH, Kim M, Billiar TR, and Seol DW. 2004 IFN-gamma enhances TRAIL-induced apoptosis through IRF-1. Eur J Biochem 271: 4222–4228. [PubMed: 15511228]
31. Schindler U, Wu P, Rothe M, Brasseur M, and McKnight SL. 1995 Components of a Stat recognition code: evidence for two layers of molecular selectivity. Immunity 2: 689–697. [PubMed: 7796300]
32. Lohoff M, Mittrucker HW, Prechtl S, Bischof S, Sommer F, Kock S, Ferrick DA, Duncan GS, Gessner A, and Mak TW. 2002 Dysregulated T helper cell differentiation in the absence of interferon regulatory factor 4. Proc Natl Acad Sci U S A 99: 11808–11812. [PubMed: 12189207]
33. Norris BA, Uebelhoer LS, Nakaya HI, Price AA, Grakoui A, and Pulendran B. 2013 Chronic but not acute virus infection induces sustained expansion of myeloid suppressor cell numbers that inhibit viral-specific T cell immunity. Immunity 38: 309–321. [PubMed: 23438822]
34. Ohmori Y, and Hamilton TA. 1997 IL-4-induced STAT6 suppresses IFN-gamma-stimulated STAT1-dependent transcription in mouse macrophages. J Immunol 159: 5474–5482. [PubMed: 9548487]
35. Goenka S, Youn J, Dzurek LM, Schindler U, Yu-Lee LY, and Boothby M. 1999 Paired Stat6 C-terminal transcription activation domains required both for inhibition of an IFN-responsive promoter and trans-activation. J Immunol 163: 4663–4672. [PubMed: 10528163]
36. Lin R, Yang L, Arguello M, Penafuerte C, and Hiscott J. 2005 A CRM1-dependent nuclear export pathway is involved in the regulation of IRF-5 subcellular localization. J Biol Chem 280: 3088–3095. [PubMed: 15556946]
37. O'Connor L, Strasser A, O'Reilly LA, Hausmann G, Adams JM, Cory S, and Huang DC. 1998 Bim: a novel member of the Bcl-2 family that promotes apoptosis. EMBO J 17: 384–395. [PubMed: 9430630]
38. Feng H, Lenarcic EM, Yamane D, Wauthier E, Mo J, Guo H, McGivern DR, Gonzalez-Lopez O, Misumi I, Reid LM, Whitmire JK, Ting JP, Duncan JA, Moorman NJ, and Lemon SM. 2017 NLRX1 promotes immediate IRF1-directed antiviral responses by limiting dsRNA-activated translational inhibition mediated by PKR. Nat Immunol 18: 1299–1309. [PubMed: 28967880]
39. Gibbons D, Fleming P, Virasami A, Michel ML, Sebire NJ, Costeloe K, Carr R, Klein N, and Hayday A. 2014 Interleukin-8 (CXCL8) production is a signatory T cell effector function of human newborn infants. Nat Med 20: 1206–1210. [PubMed: 25242415]
40. Das A, Rouault-Pierre K, Kamdar S, Gomez-Tourino I, Wood K, Donaldson I, Mein CA, Bonnet D, Hayday AC, and Gibbons DL. 2017 Adaptive from Innate: Human IFN-gamma(+)CD4(+) T Cells Can Arise Directly from CXCL8-Producing Recent Thymic Emigrants in Babies and Adults. J Immunol 199: 1696–1705. [PubMed: 28754679]

41. Kollmann TR, Levy O, Montgomery RR, and Goriely S. 2012 Innate immune function by Toll-like receptors: distinct responses in newborns and the elderly. Immunity 37: 771–783. [PubMed: 23159225]

42. Kollmann TR, Kampmann B, Mazmanian SK, Marchant A, and Levy O. 2017 Protecting the Newborn and Young Infant from Infectious Diseases: Lessons from Immune Ontogeny. Immunity 46: 350–363. [PubMed: 28329702]

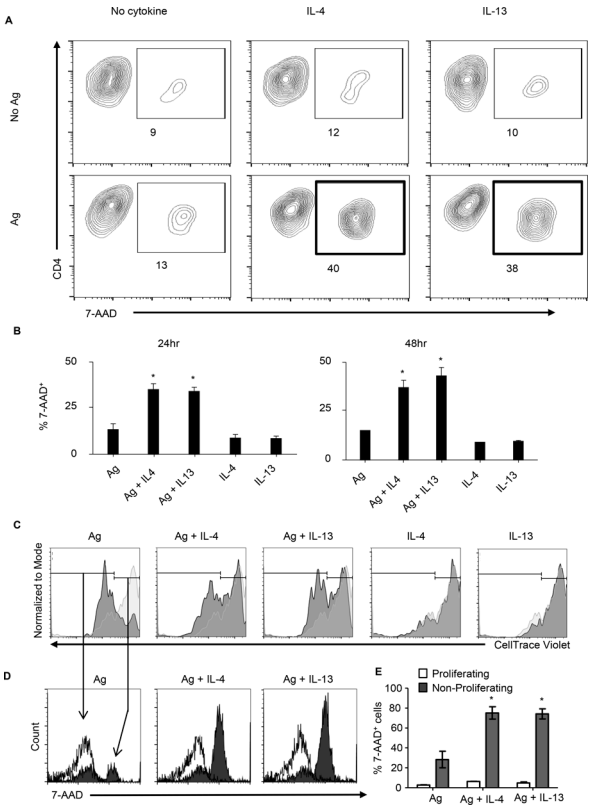

Figure 1. Cytokine-induced Th1 death is dependent on stimulation with Ag.

(A, B) Sorted HR^+CD4^+ neonatal Th1 cells were stimulated with anti-CD3/anti-CD28 antibodies (Ag) in the presence or absence of recombinant murine IL-4 or IL-13 (5U each) and cell death was measured by 7-AAD staining of $CD4^+$ T cells. Unstimulated (no Ag) cells were used as control. (A) shows a representative experiment for 7-AAD binding after 24 hours incubation with numbers indicating the % of $7\text{-}AAD^+$ cells. (B) Shows 7-AAD binding data combined from 3 independent experiments performed for 24 or 48 hours. The bars represent the mean percentage ± SEM of $7\text{-}AAD^+CD4^+$ T cells. $*p < 0.05$ as determined by one-way ANOVA with Bonferroni post-test. The stars indicate significant difference between stimulation with Ag and cytokine relative to stimulation with Ag or cytokine alone. (C, D) Sorted HR^+CD4^+ neonatal Th1 cells were labelled with CellTrace Violet and stimulated with Ag and cytokines for 72 hours. The cells were then assessed for proliferation by analysis of dye dilution (C) and cell death by 7-AAD labeling (D, E). In C, the light grey histograms represent unstimulated cells as reference for dye labeling. The dark grey histograms show dye dilution as consequence of Ag and cytokine stimulation. (D) Shows 7-AAD incorporation by proliferative and non-proliferative cells. (E) Shows the mean ± percentage of $7\text{-}AAD^+$ cells among the proliferating and non-proliferating lymphocyte. The stars represent a significant difference relative to Ag treated cells using an ANOVA with Bonferroni post-test.

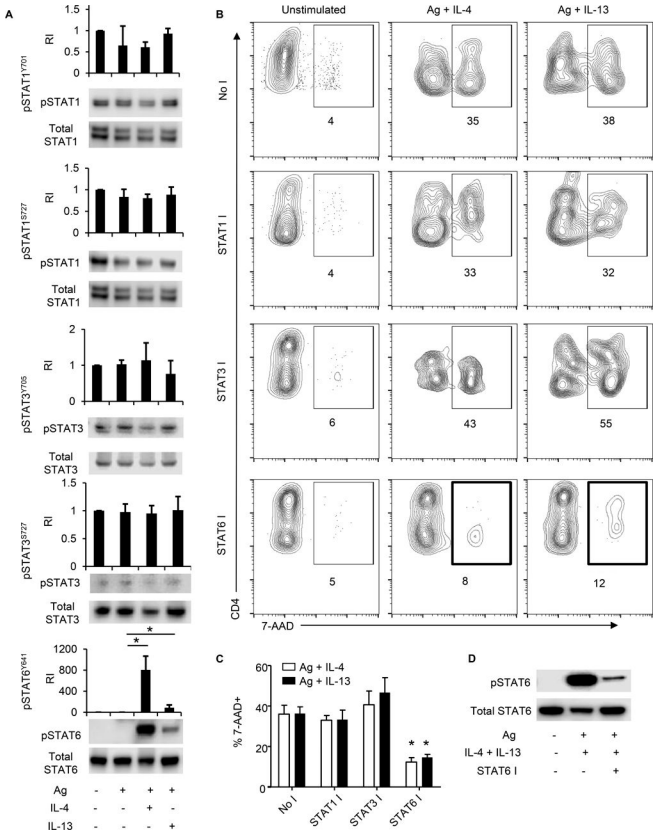

Figure 2. Stimulation with Ag and cytokines induces STAT6 phosphorylation in dying Th1 cells.

(A) Sorted HR^+CD4^+ neonatal Th1 cells were stimulated with Ag and cytokines as in Fig. 2 and used to measure STAT phosphorylation after 20 (STAT1 and STAT3) or 60 (STAT6) min by Western blot. The upper bands in each blot represent phosphorylated STAT molecules while the lower bands represent total STAT proteins. The graphs show the relative band intensity (RI) as a ratio of pSTAT over total STAT. Each bar represents the mean RI ± SEM data compiled from three independent experiments. $*p < 0.05$ as determined by one-way ANOVA with Bonferroni post-test. (B, C) Sorted HR^+CD4^+ neonatal Th1 cells were pre-incubated with STAT inhibitors (STAT I) for 60 min, Ag plus cytokines were added for stimulation as in (A), and apoptosis was measured by 7-AAD staining of $CD4^+$ T cells after 48h incubation. (B) Shows a representative experiment for 7-AAD binding with numbers indicating the % of 7-AAD^+ cells. (C) Shows apoptosis data compiled from three independent experiments. Each bar represents the mean percent 7-AAD^+ cells ± SEM. $*p < 0.05$ as determined by one-way ANOVA with Bonferroni post-test. (D) Shows phosphorylated (pSTAT6) and total STAT6 levels in HR^+CD4^+ neonatal Th1 cells that were stimulated as indicated.

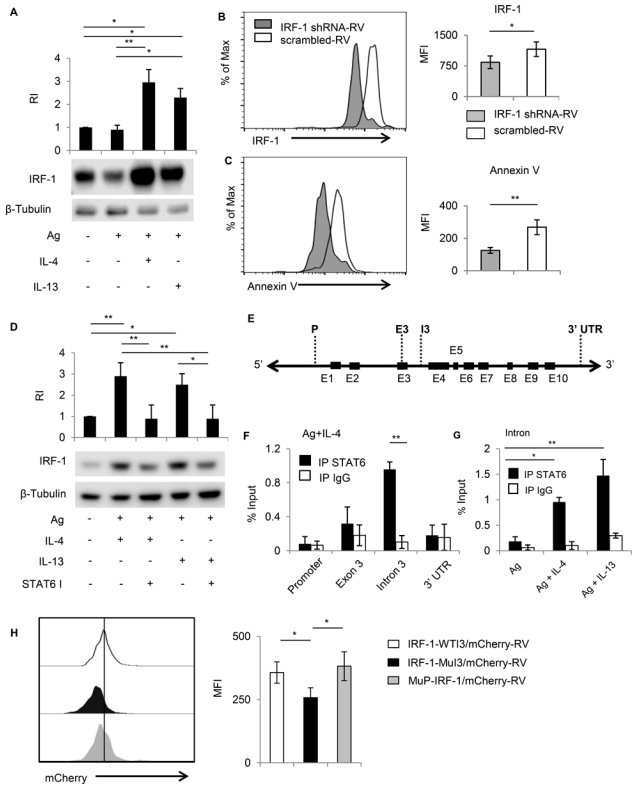

Figure 3. STAT6-mediated IRF-1 upregulation is required for Th1 cells to undergo apoptosis.

(A) Sorted HR^+CD4^+ neonatal Th1 cells were stimulated with Ag and cytokines and the cells were used to measure IRF-1 protein expression by Western Blot. The upper bands represent IRF-1 expression while the lower bands represent β-Tubulin control. Each bar represents the mean RI ± SEM data compiled from three independent experiments. *p <0.05, **p <0.01 as determined by one-way ANOVA with Bonferroni post-test. (B, C) Sorted HR^+CD4^+ neonatal Th1 cells transduced with a retroviral vector (RV) containing a cocktail of 3 different IRF-targeting shRNA molecules were stimulated with Ag + IL-4 and assessed for IRF-1 upregulation (B) and Annexin V binding (C). Cells that were transduced with RV containing scrambled shRNA were used as control. The histograms show a representative experiment for IRF-1 expression and Annexin V binding. The bars represent the mean MFI ± SEM data compiled from three independent experiments where *p < 0.05, **p < 0.01 as analyzed by Student t-test. (D) Shows IRF-1 expression by HR^+CD4^+ neonatal Th1 cells that were stimulated with Ag and cytokines in the presence or absence of STAT6 I. *p <0.05, **p <0.01 as determined by one-way ANOVA with Bonferroni post-test. (E) Shows a schematic diagram of the murine IRF-1 locus with the dotted lines indicating potential STAT6 binding sites ($TTC(N_{3-4})GAA$) within the promoter region (P), exon 3 (E3), intron 3 (I3), and the 3' UTR. In (F, G) Sorted HR^+CD4^+ neonatal Th1 cells were stimulated with antigen and cytokines and STAT6 binding to the IRF-1 gene was evaluated by ChIP followed by PCR. (F) shows binding to the 4 potential sites identified in (E) while (G) Shows binding to I3 site triggered by IL-4 and IL-13. * p<0.05 and ** p<0.01 as determined by Student t-test (F) and one-way ANOVA with a Bonferroni post-test (G). (H), HR^+CD4^+ neonatal Th1 cells were transduced with IRF-1/mCherry-RV carrying wild type

(IRF-1-WTI3/mCherry-RV) or mutated (IRF-1-MuI3/mCherry-RV) STAT6 I3 binding site and the cells were analyzed for mCherry fluorescence as a readout for IRF-1 expression upon stimulation with Ag and IL-4. Cells transduced with IRF-1/mCherry RV carrying mutated STAT6 binding sequence within the Promoter (MuP-IRF-1/mCherry-RV) were used for control purposes. The left panel shows histograms of IRF-1 (mCherry) fluorescence and the right panel shows the corresponding MFIs. *p <0.05 as determined by one-way ANOVA with Bonferroni post-test.

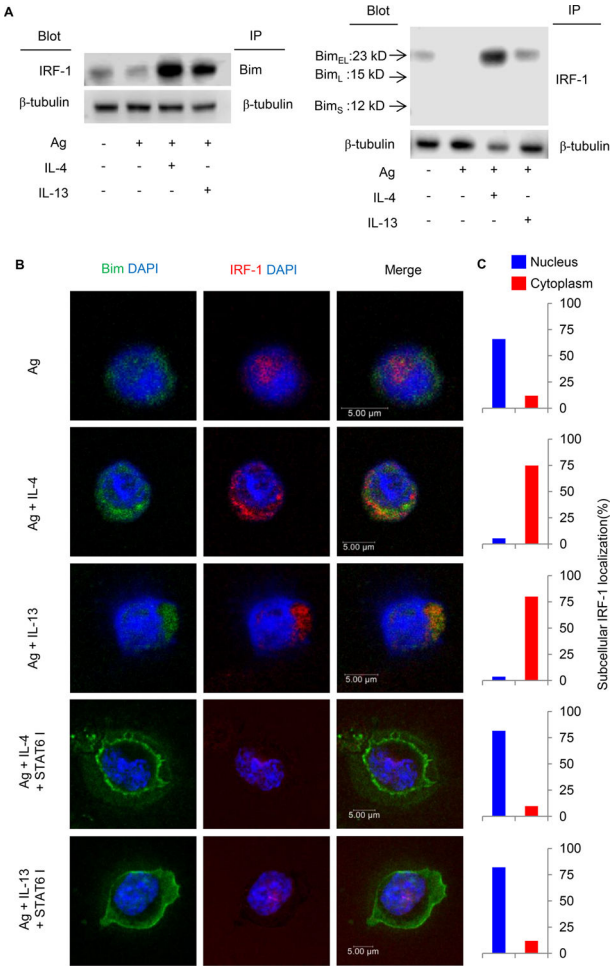

Figure 4. IRF-1 co-localizes with Bim in the cytoplasm in a STAT6-dependent manner to drive neonatal Th1 apoptosis.

(A) Shows a pull-down assay of IRF-1 and Bim in lysates of HR^+CD4^+ neonatal Th1 cells stimulated with diluent or Ag and cytokines. The left blot shows immunoprecipitation (IP) with anti-Bim antibody and blotting with anti- IRF-1 antibody whereas the right blot shows the reverse. In each blot, an IP and blotting with anti-β Tubulin antibody was included as a loading control. (B) HR^+CD4^+ neonatal Th1 cells were stimulated with Ag alone (Ag), Ag +IL-4, Ag+IL-13, Ag+IL-4+STAT6 I, or Ag+IL-13+STAT6 I for 24 hours. The images were obtained by staining with anti-Bim (green) and anti-IRF-1 (red) antibodies along with DAPI. The scale bars represent 5 µm. (C) Shows compiled imaging data from two independent experiments. Each bar represents the percent cells with the indicated subcellular localization of IRF-1. At least 100 cells were analyzed for each stimulation.

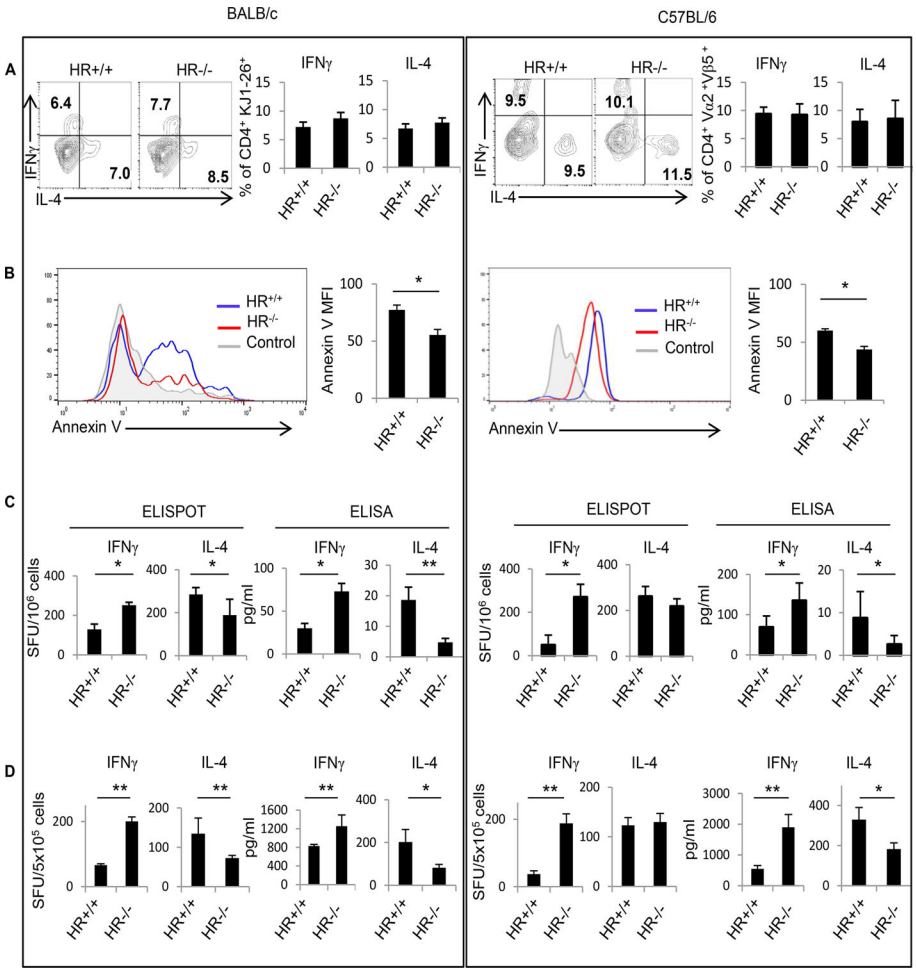

Figure 5. HR$^{-/-}$ mice yield apoptosis resistant Th1 cells leading to balanced Th1/Th2 secondary responses both in Balb/c and C57BL/6 mouse strains.

One day-old (neonatal) HR$^{+/+}$ Balb/c (H-2^{d}) and C57BL/6 (H-2^{b}) host mice were given intravenously (i.v.) through the facial vein spleen T cells from neonatal HR$^{-/-}$ or HR$^{+/+}$ DO11.10 (H-2^{d}) and OT-II (H-2^{b}) donor mice, respectively. The host mice were then given intraperitoneally (i.p.), within 24 hours of T cell transfer, Ig-OVA, an Ig carrying OVAp which incorporates both DO11.10 and OT-II epitopes. On day 14, the spleen cells were harvested and the responder DO11.10 and OT-II T cells were tracked with KJ1–26 (DO11.10 T cells) and Vα2/Vβ5 (OT-II T cells) TCR-specific antibodies and analyzed for ex-vivo primary (A), Th1 apoptotic (B) and in vitro recall (C) responses. (A) The contour plots show representative intracellular IFNγ (Th1) and IL-4 (Th2) ex-vivo responses and the bar graphs show results combined from 3 independent experiments. Each bar represents mean ± SEM. (B) The spleen cells from both strains were stimulated with OVAp and apoptosis of Th1 cells was measured by Annexin V staining on CD4^{+}KJ1–26^{+}IFNγ^{+} DO11.10 cells and CD4^{+}Vβ5^{high}Vα2^{high}IFNγ^{+} OT-II cells. The histograms show representative experiments and the bar graphs show MFI ± SEM of Annexin binding compiled from 3 independent experiments. The no Annexin V (control) staining was used as an auto fluorescence negative control. (C) For analysis of the recall response, the spleen cells from both strains were stimulated with OVAp for 24 hours and cytokine secretion was

measured by both ELISPOT and ELISA. Each bar represents the mean ± SEM of spot forming units (SFU) or pg/ml cytokines compiled from 3 independent experiments. (D) For analysis of the secondary response, the mice were challenged with OVAp in CFA 2 months after priming with Ig-OVA. Ten days later, IFNγ and IL-4 LN responses were measured by ELISPOT and ELISA after in vitro stimulation with OVAp. The bars represent data compiled from three independent experiments. *$p < 0.05$, **$p < 0.01$ as analyzed by Student t-test.

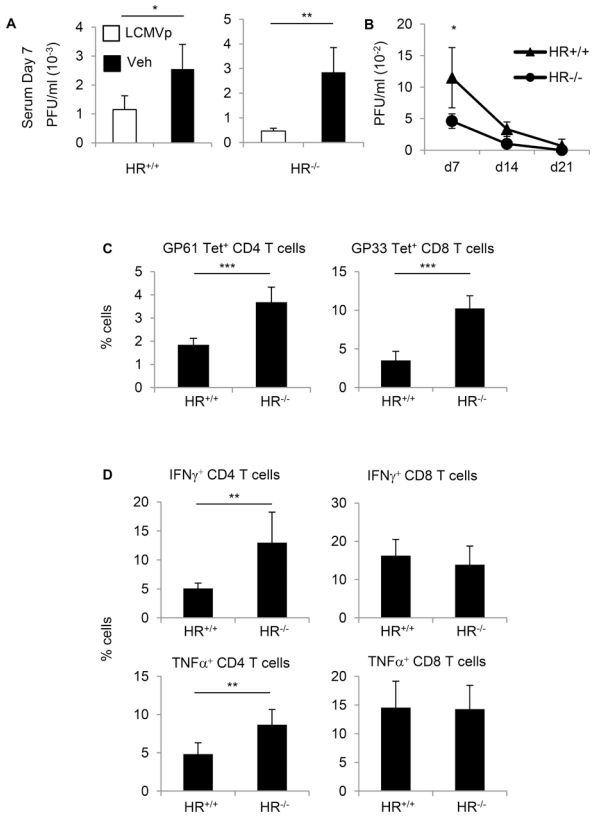

Figure 6. Vaccinated HR$^{-/-}$ neonatal mice develop enhanced Th1 responses and resist chronic LCMV Clone 13 infection.

Neonatal HR$^{+/+}$ and HR$^{-/-}$ C57BL/6 mice were immunized i.p. with an LCMVp vaccine consisting of a mixture of LCMV GP33–41 and GP61–80 peptides (10 μg each). Seven weeks later, the mice were infected with 2×10^6 pfu LCMV CL13. Groups of mice that were not vaccinated (Veh) but infected with CL13 at seven weeks of age were included for control purposes. (A) Shows virus titers in serum 7 days after infection. (B) Shows a comparison of viral titers in LCMVp-vaccinated HR$^{+/+}$ relative to HR$^{-/-}$ mice at days 7, 14, and 21 post infection. (C) Shows the percentage of GP61Tet$^+$CD4$^+$ cells among total CD4 T lymphocytes and GP33Tet$^+$CD8$^+$ cells among total CD8 T cells at the conclusion of viral titer analyses. (D) shows the percentages of IFNγ- and TNFα-producing CD4 and CD8 T cells. *$p < 0.05$, **$p < 0.01$, ***$p < 0.001$ as analyzed by Student t-test

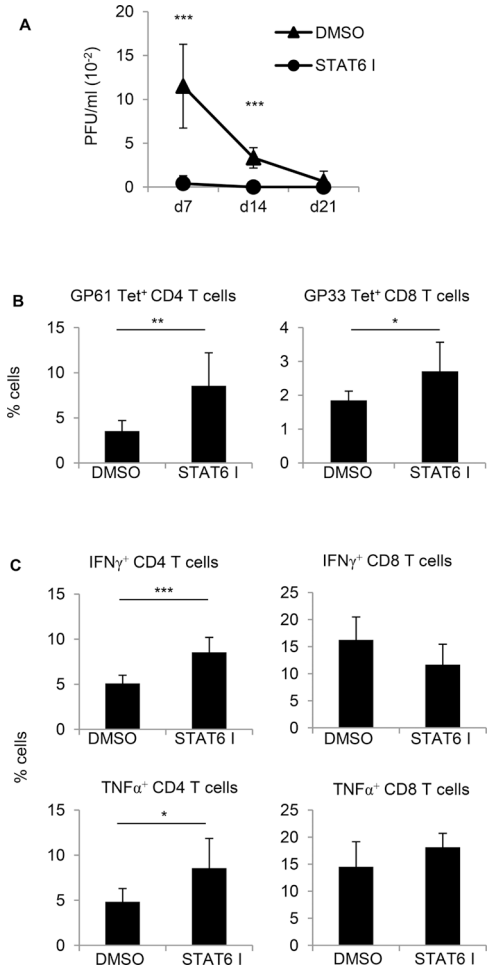

Figure 7. Inhibition of STAT6 activation during viral challenge of neonatally vaccinated HR$^{+/+}$ mice restores Th1 responses and protects against LCMV Clone 13 infection.

Neonatal IL-13Rα1$^{+/+}$ (HR$^{+/+}$) C57BL/6 mice were vaccinated i.p. with LCMV GP33–41 and GP61–80 peptides (10 μg each) in IFA at day 3 of age. Seven weeks later, the mice were divided into 2 groups one of which received STAT6 inhibitor (STAT6 I) daily for 5 days and the other served as vehicle control (DMSO). The mice were infected i.v. with 2 ×10^6 pfu LCMV CL13 on day 3 of STAT 6 I treatment. (A) Shows a comparison of viral titers in serum of mice vaccinated with LCMVp and untreated (DMSO) or treated with STAT6 I at days 7, 14, and 21 post infection. Six weeks post infection the splenic T cell responses were measured upon stimulation with GP33/61 peptides *in vitro*. The frequency of GP61Tet$^+$CD4$^+$ and GP33Tet$^+$CD8$^+$ cells were measured alongside intracellular IFNγ and TNFα production. (B) Shows the percentage of GP61Tet$^+$CD4$^+$ cells among total CD4 T lymphocytes and GP33Tet$^+$CD8$^+$ cells among total CD8 T cells. (C) shows the percentages of IFNγ- and TNFα-producing CD4 and CD8 T cells in STAT6 I treated and untreated (Nil) mice.